Acc. Chem. Res. **1998,** *31,* 699−707

ARTICLES

Laser Temperature Jump Induced Protein Refolding†

MARTIN GRUEBELE,* JOBIAH SABELKO, RICHARD BALLEW, AND JOHN ERVIN

Department of Chemistry and Beckman Institute for Advanced Science and Technology, University of Illinois, Urbana, Illinois 61801

Received October 20, 1997

I. Introduction

Small-molecule reaction mechanisms are now well-understood primarily because of the highly directed and often localized nature of covalent bonds, whose strength greatly exceeds k_BT. The same cannot be said for protein folding, which involves numerous cooperative noncovalent interactions whose individual magnitudes can be less than a single kilojoule per mole, leading to a complex, locally random-looking free energy "landscape".[1,2] Protein energetics challenge "conquer-and-divide" strategies, which aim to partition energy changes into energetically comparable contributions from hydrophobic, hydrogen bonding, salt bridge, surface solvation, and other effects, although hydrophobic interactions have emerged as the major factor leading to compact structures.[3] With overall free energies of stabilization on the order of only tens of kilojoule per mole, solvent structure is no longer a perturbation but a critical part of enthalpic and entropic contributions to the free energy.[4]

During the past 15 years, protein folding experiments have made a transition from mainly structure/thermodynamics to including extensive kinetic studies.[5−13] Why look at dynamical events? They are our most direct window on mechanism, allowing us to study transition states, energetically "downhill" formation of structure, intermediates, and traps as they form and decay. Although it might be possible in principle to deduce structure merely by an examination of the amino acid sequence, the sequence−structure problem is further illuminated by knowledge of the protein backbone folding motions, the temporal sequence of contacts formed, and hence the dynamical hierarchy of structural elements.

As discussed later, kinetic studies must build on a firm basis of structural and thermodynamic information, much like what has happened in organic chemistry earlier. X-ray and NMR structures provide indispensable information about the initial and final states of kinetic studies. Time-resolved techniques generally determine only partial structural information (e.g. approximate amino acid−quencher separation in fluorescence). Steady-state studies under a variety of solvent conditions can be used to characterize a steady-state folding "phase diagram", which provides starting points for time-resolved folding experiments. However, care must be taken before states in such a phase diagram are identified with transient intermediates during the actual refolding process.[14]

Kinetic experiments must somehow initiate either a folding or an unfolding reaction and then monitor changes in some property of the system. Stopped-flow mixing, coupled with circular dichroic (secondary structure),[15] fluorescence (tertiary structure),[16] or NMR amide proton exchange measurements (secondary structure),[17] has been very successful in the hands of protein kineticists. In many cases, such experiments have shown nascent phases within the 2−5 ms dead-time of a stopped-flow apparatus: Some proteins manage to regain a significant degree of nativelike tertiary[6] or secondary[18] structure in less than a few milliseconds.

It is this very efficient protein folding which piqued our interest several years ago. Could it be that many slow phases of folding are in fact "escape attempts" of kinetically trapped misfolded proteins over large activation barriers (e.g. due to proline isomerization)? Could it be that a fraction of the folding ensemble proceeds either to the native state or to a "late" folding intermediate very rapidly, in some cases even without an activation barrier?[19]

Lower time limits are set by the fastest possible formation of local structure—either secondary, such as isolated α-helices (≈100 ns)[20,21] and β-turns (6 μs),[22] or tertiary, such as small loops (≈1 μs).[23] Observation of folding near these time scales demanded new approaches for detection and the development of faster techniques to stimulate the folding reaction.[7−9,11−14,21−27]

We have chosen temperature as the parameter to control folding because the folding free energy of proteins depends strongly on temperature. Proteins melt upon cooling as well as upon heating of their aqueous solu-

Martin Gruebele received his Ph.D. from the University of California at Berkeley in 1988 and joined the faculty at the University of Illinois in 1992 after a postdoctoral fellowship at Caltech.

Jobiah Sabelko received his B.S. in chemistry from the University of Wisconsin, Eau Claire, in 1994. He is currently working on his Ph.D. at the University of Illinois Urbana-Champaign.

Richard Ballew received his Ph.D. from the University of Illinois at Urbana−Champaign in 1996. He is currently employed as a research scientist at CuraGen Corp.

John Ervin received his B.A. in chemistry from Cornell University in 1994. After working with Perseptive Biosytems, he joined the Ph.D. program at the University of Illinois.

† Abbreviations: T-Jump, temperature jump; apoMb, apomyoglobin; *pc*-apoMb, (*physeter catodon*) sperm-whale apomyoglobin; *eq*-apoMb, (*equine*) horse-apomyoglobin; PGK, phosphoglycerate kinase; GuHCl, guanidinium hydrochloride.

10.1021/ar970083x CCC: $15.00
Published on Web 08/08/1998

tions.[28,29] Configurational entropy is responsible for the latter, while cancellation of the "hydrophobic effect" due to solvent reorganization at low temperatures is responsible for the opening of protein cores upon cooling.[30,31]

An upward temperature jump can thus be used to induce rapid *re*folding from cold-denatured states or rapid *un*folding to heat-denatured states. Pioneering work in the 1950s set the stage for such studies on the microsecond time scale: resistive T-jumps have been widely employed in the study of low-ionic strength reaction kinetics since the development of the Eigen relaxation machine.[32] Twenty years later the groundwork was laid for the nanosecond time scale: the first laser T-jumps directly heating water to study organic reactions were realized by Flynn and co-workers.[33]

The Cambridge group (see Account in this issue) has applied the Eigen technique to study the transition state via effects of amino acid mutations on refolding rates.[34] The Los Alamos, New York,[12,21] Pennsylvania,[26] and NIH[22] groups have used laser T-jumps to probe peptide dynamics and protein unfolding on time scales from picoseconds to milliseconds (see Accounts in this issue). Our group has used laser T-jumps to investigate refolding of proteins from the cold denatured state.[9,31,35−37]

II. Time-Resolved Technique

Advances in laser technology have made T-jumps on a nanosecond or picosecond time scale robust experiments.[9,22,26,36] Initial attempts were hampered by the minuscule absorbance of most solvents at visible/near-IR wavelengths. Dyes which absorb and redistribute laser energy to the solvent produce large T-jumps but can introduce complications due to sample−dye interactions. This problem was elegantly bypassed by Flynn and co-workers who used Raman-shifted light to directly heat the solvent.[33]

Our modern version of the T-jump apparatus is shown in Figure 1.[36] Protein samples are placed in an aqueous buffer and denatured by supercooling to temperatures as low as −15 to −20 °C. Fast heating is achieved using Raman shifted IR pulses from a methane cell in a carefully optimized pumping geometry. Longer path lengths in the sample are made possible by splitting the heating beam into two counterpropagating parts, resulting in a nearly constant longitudinal heating profile in the 0.3−0.5 mm path length capillary cells.

Pumping the OH overtone of water with 1.54 μm Raman light thermalizes the solvent within 100 ps (<10 ns duration of our heating pulse).[38] This suddenly leaves the unfolded protein backbone, which cannot respond with large amplitude motions on such a short time scale,[23] under thermodynamic conditions where refolding is favorable. T-jumps up to 30 °C are possible, producing easily observed population changes (Figures 2 and 4), although the jump still corresponds to only $\approx {}^1/_{10}\ k_BT$. Jumping near the 4 °C density maximum of water reduces the interference from compression waves.[36] Care must nonetheless be taken to avoid interference from such effects (see section IV). Our technique allows a wide range of solvent conditions, from pure water to aqueous solutions of varying ionic, denaturant, glycerol, helix inducer, or fluorescence quencher concentrations, and on to organic solvents.

After refolding is triggered, protein conformational changes must be monitored. Raman,[39] infrared,[12,26] absorption,[27] NMR line width,[7] and fluorescence[8,11,34] techniques have been adapted to fast folding experiments. We use tryptophan fluorescence induced by an ultraviolet (280−295 nm) train of pulses spaced 14 ns apart (Figure 1). This mode-locked pulse train is able to record the entire history of protein folding motions in a single sweep. Expensive engineered protein samples need not be flowed (picomole/microliter quantities of <20 μL are possible), and reproducibility of the T-jump (although good) is not an issue.

The resulting series of fluorescence decays is detected by a picosecond photomultiplier and digitized (Figure 1). A typical 20 ns to 2 ms folding data set contains ≈100 000 fluorescence decays and their evolving intensity and lifetime characteristics. Here we use a compact "model-free" representation of the data in terms of the quantity χ_2. f_1 denotes the fluorescence decay of the unfolded protein, and f_2, the fluorescence decay of the final protein state (native or a partially refolded reference state). Then fluorescence transients at any time during folding can be approximately represented as

$$f(t) = a_1(t)f_1 + a_2(t)f_2, \quad \chi_2(t) = a_2(t)/(a_1(t) + a_2(t)) \quad (1)$$

χ_2 measures whether the fluorescence closely resembles the unfolded state ($\chi_2 = 0$) or the final state ($\chi_2 = 1$).[9] This is essentially equivalent to representing the data in terms of two components of a singular-value decomposition (SVD).[31] A detailed analysis in terms of fluorescence lifetimes/intensities or higher order SVD components is also possible.

Fluorescence experiments can be designed in several complementary ways.[8,9,16,40] One elegant approach makes use of the fact that, without a dominant quenching mechanism, fluorescence tends to capture most or all of the kinetic phases. Small rate changes upon site-directed mutagenesis then allow one to infer the effect of specific residues on the transition-state energy.[8]

In our approach, a dominant tryptophan quenching interaction is used as a direct structural marker. Two kinds of probes may be present or may be introduced into the protein by mutagenesis. Förster quenching by heme, dansylated residues or nitrosated tyrosines can measure distance variations in the 10 to >40 Å range due to the $1/r^6$ dependence of this type of quenching.[22,41] Dexter quenching by histidine, cysteine, or methionine residues[42−44] has an exponential distance dependence sensitive to the 3−8 Å range. Carefully chosen tryptophan−quencher pairs therefore can yield direct structural information.[41]

As for NMR NOE's (also a $1/r^6$ measure), a number of such distance probes should ideally be introduced to

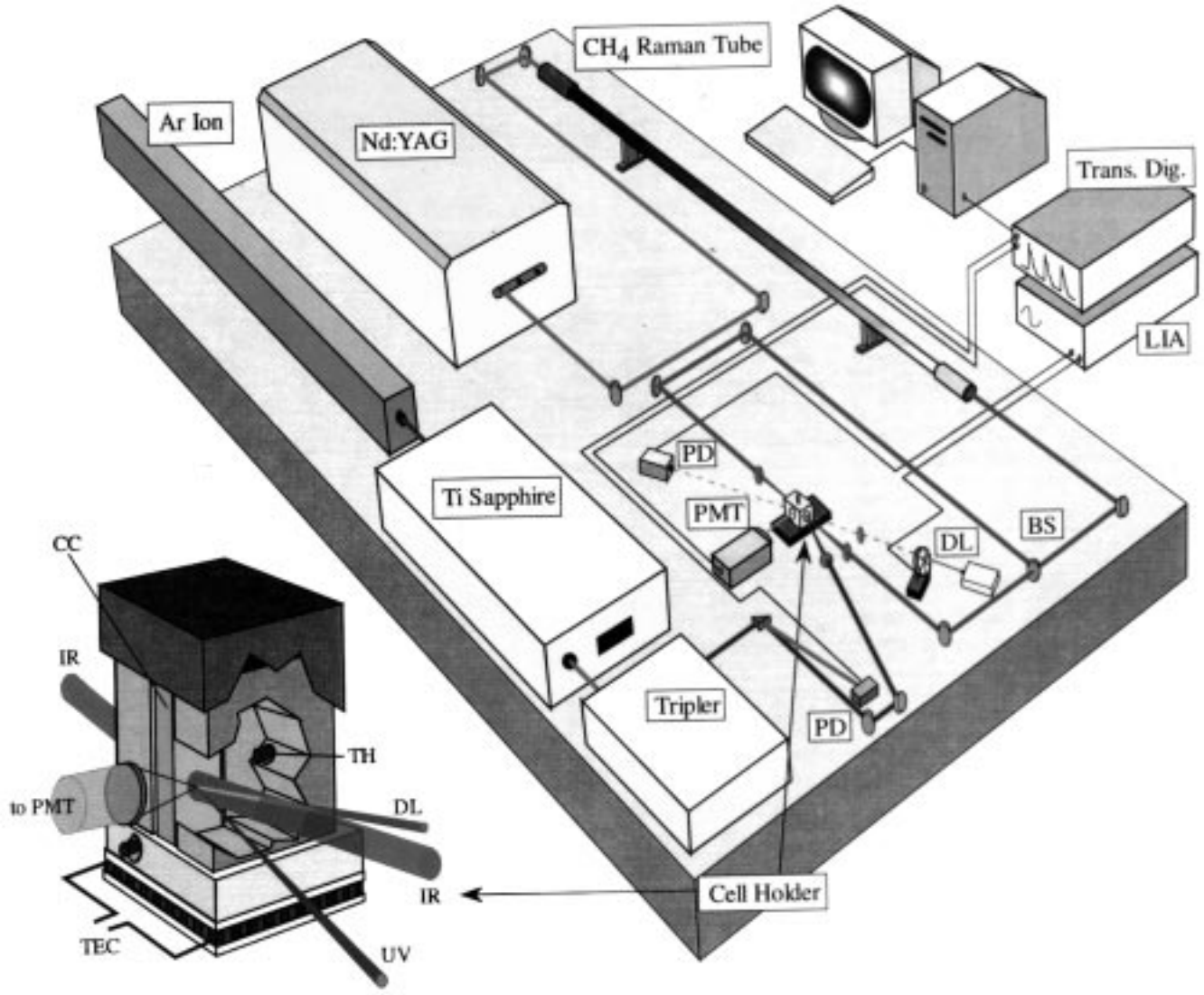

FIGURE 1. Single sweep laser T-jump apparatus as described in Ballew et al.[36] The output of a Nd:YAG laser is imaged into a 180 cm Raman cell. The resulting 1.5 μm heating pulse is split into two components by a beam splitter (BS) and imaged onto the sample capillary. At the same time, a 14 ns spaced pulse train from a frequency-tripled mode-locked titanium:sapphire laser is gated into the sample cell. A fast photomultiplier (PMT) detects the resulting fluorescence train. The data are digitized (Trans. Dig.) at 500 ps intervals. The digitizer sampling rate is locked to the titanium:sapphire laser cavity by a photodiode sampling the laser output (PD bottom). The magnitude of the T-jump is monitored by feeding the absorbance changes of the aqueous solvent, detected by another photodiode (PD top), to a lock-in amplifier (LIA). Also shown is a sample cell with insulated block and sample capillary (CC) cooled by a thermoelectric cooler (TEC) with feedback loop. Steady-state temperature is monitored by several thermistors (TH) at and below the beam height. IR beams heat the sample, UV pulses of much smaller diameter probe the fluorescence, and the diode laser (DL) probes the temperature jump.

constrain the dynamical variations of structure during folding. This will be a future direction in our studies. In our approach, small amounts of sample aggregation or small differences in sample preparation are of no consequence because the rates themselves (e.g. $k_{obs} = k_+ + k_-$ for the simplest reversible denatured $\rightleftarrows$ folded reaction), and not their differences, are of interest.

As seen in section IV, even in the presence of a dominant quenching mechanism, nonspecific interactions such as solvent quenching can also be judiciously tuned to extract further structural information. Ideally, one would also like to collect simultaneous wavelength-dispersed fluorescence to gain direct time-resolved information on tryptophan solvent exposure (typically $\lambda_{max} =$ 330 nm in the core, 350 nm when solvent exposed), but this remains to be implemented in submicrosecond resolution folding experiments.

III. Unfolded Ensemble and Folding Free Energy Surface

Immediately following the T-jump, the backbone structure has not responded with large amplitude motions, due to protein size and solvent viscosity.[13,23] The subsequent observed protein refolding kinetics therefore depend critically on the nature of this initial ensemble.

Numerous proteins, including apoMb (apomyoglobin, the heme-free proto-myoglobin), cytochrome *c*,[45] and PGK (phosphoglycerate kinase) cold denature under appropriately chosen conditions (Table 1).[46,47] Water is more

Table 1. Three Illustrative Examples of the Time Scales Monitored by Fast Laser T-Jump Refolding from the Cold Denatured State[a]

protein	fast phases	observed variables	conditions	refs
apomyoglobin (horse)	250 ns prot, 4−17 μs qu	χ_2 and I_{tot}	pH 5.9, 10 mM PO_4^{3-}	9, 34, 38
cytochrome *c* (yeast iso 1)	6 μs qu by 25%	I_{tot}	pH 2.2, 5 mM KCl	40
phosphoglycerate kinase (yeast)	several 10 μs to 6 ms qu	χ_2	pH 6.15, 20 mM PO_4^{3-}, 1mM EDTA, 1 mM DTT, 200 mM GuHCl	40, 84

[a] "Prot" indicates a protective phase where fluorescence increases as a function of time, whereas "qu" indicates that the fluorescence is being quenched as a function of time. χ_2 is defined in eq 1.

ordered around hydrophobic than hydrophilic residues,[30] resulting in disruption of the tertiary structure of proteins at low temperature, although residual tertiary and secondary structure can persist.[29] In other cases, nearly complete loss of secondary structure has been reported upon cold denaturation.[47,48]

Figure 2 schematically depicts the solvated protein free energy as a function of temperature T and reaction coordinates Rs. "Rs" stands for a collection of reaction coordinates because $\Delta G(\mathrm{Rs},T)$ cannot necessarily be interpreted in terms of a single reaction coordinate (e.g. radius of gyration, number of native contacts, etc.). At low temperatures, there may be only a single basin corresponding to a denatured state D_C; as T increases, the native basin grows deeper, leading to a high equilibrium fraction of native protein N. At yet higher temperature, the denatured basin will grow deeper again and the heat denatured ensemble D_H is populated.

The nanosecond T-jump promotes D_C to an ensemble with nearly identical distributions of Rs because the protein backbone cannot respond with large-amplitude motions on time scales under a few nanoseconds. The thermodynamically favored state is now the native state N. Depending on the location of the promoted ensemble with respect to the folding barrier, the population may proceed directly to the native state via downhill "type 0" kinetics or to a new unfolded ensemble, which then refolds over the barrier via activated "type 1" kinetics (Figure 2).[49] The "folding funnel" picture[50] also allows for entirely type 0 kinetics with no significant barrier. In practice, this depends on how configurational entropy (the "width" of the funnel) balances out enthalpy changes (the "depth" of the funnel) during folding.

Structural cartoons for U_{RC} (random coil), D_C, and N are shown for *eq*-apoMb in Figure 2. N contains well-characterized structure, including hydrophobic cores consisting of helices ABGH and CDE (Figure 2).[51,52] The weak CDE core easily denatures under many conditions.[6,53−55] In the cold-denatured ensemble of *eq*-apoMb,[56] even the strong AGH core is disrupted.[31] Investigation of the fluorescence (due to Trp 7 and 14 in the A helix) shows that the A-helix Trp residues become exposed to solvent (Figure 3), while the CD spectrum approaches a helicity comparable to the helix content of GH only (Figure 4).[31] An investigation of horse apoMb and its A-helix peptide by multiple techniques further supports a concerted two-state $D_C \rightleftarrows N$ transition with only some GH structure left in D_C.[31] Therefore the initial D_C ensemble consists of a small amount of native protein, which is not much affected by the T-jump, and a large amount of cold-denatured protein, which refolds after the T-jump. The initial ensemble is not a heterogeneous collection of protein molecules of intermediate secondary structure content.

PGK is an example of a protein which thoroughly cold denatures.[47] At higher GuHCl concentrations, cold denaturation results in an almost complete loss of secondary structure.[57] Many other proteins can be cold-denatured, and site-directed mutagenesis offers the potential for even greater variety.

IV. Fast Refolding Ensemble

Following the temperature jump, refolding is monitored in our experiments by changes in the protein fluorescence due to the appearance of quenching interactions. We start with a brief general discussion of three examples summarized in Table 1, to illustrate the possibilities within reach of fast T-jump refolding experiments. We then discuss in more detail the folding of apoMb using the data shown in Figure 4.[9,35]

Yeast cytochrome *c* can be partially cold-denatured at pH 2.2 under low-salt conditions, near its acid-unfolding transition. In the native state, a single tryptophan residue in position 59 is strongly Förster quenched by the covalently attached heme group but fluoresces more in the unfolded state.[58] A number of electrochemically[25] and mixing[39,59−61] induced fast folding experiments have shown complex ligand-binding dynamics on a 100 μs and longer time scale. Cytochrome *c* has also been studied at high GuHCl concentrations, leading to an estimate for diffusional contact formation in proteins on the order of 1 μs (short loops) to 40 μs ($\approx$60 residue loop).[13,23] Our result shows a single-exponential phase (25% fluorescence intensity quenching, $\approx$15% population change) of 6 μs, illustrating the power of specific tryptophan−heme quenching interactions. The fast collapse takes place under acidic conditions where histidine−heme binding is unimportant; it is probably a barrier-free size reduction and sets the stage for further folding events by greatly reducing the conformational search space of the protein.[59]

Phosphoglycerate kinase is a 415 residue two-domain enzyme. Experiments by Beechem and co-workers have shown that, in the 5 ms dead-time of their experiment, PGK collapses to a globular state with donor−acceptor distances that can be shorter (*inter*domain) or longer (*intra*domain) than in the native state.[40,62,63] NMR studies also show extensive amide protection (indicative of secondary structure) in the millisecond dead-time of the experiment.[18] In the presence of GuHCl, the cold-

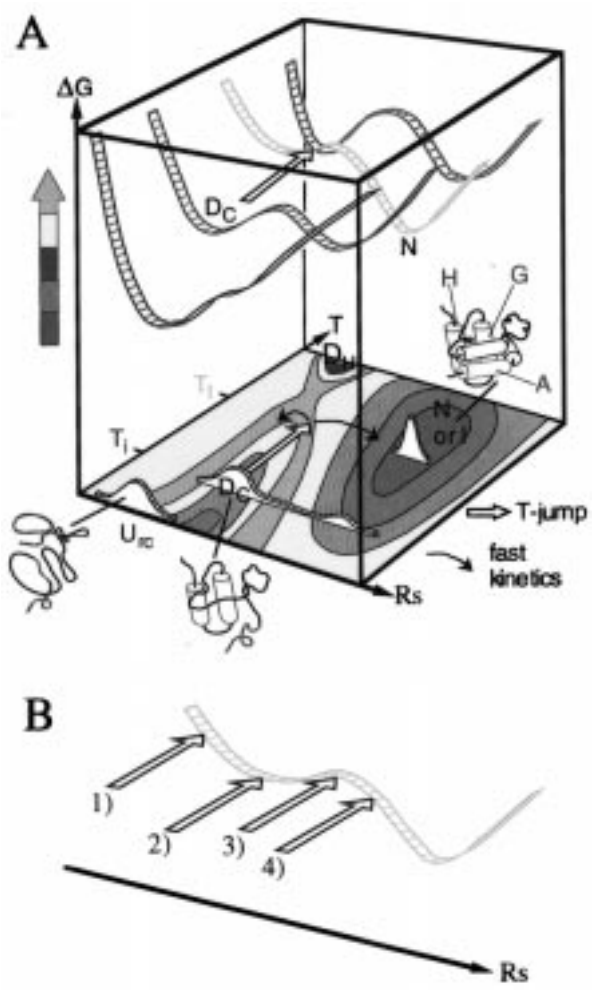

FIGURE 2. (A) Schematic free energy diagram showing relevant protein ensembles together with possible dynamics following a T-jump. Top "strips" show the free energy as a function of reaction coordinates Rs at four temperatures. A contour plot of the complete function $\Delta G(T,\mathrm{Rs})$ is shown at the bottom. It is important that Rs not be mistaken for a single reaction coordinate: protein folding can often *not* be explained by a single reaction coordinate.[4,73] Under our cold-denaturation conditions, the denatured basin and native basin are of comparable depth, resulting in population of both D_C and N states. D_C is substantially denatured, but not a random coil U_{RC}. This will be true for some proteins, while for others (e.g. PGK) D_C and U_{RC} are substantially similar. After the T-jump (white arrow), the native basin is deepest and the protein sample refolds. The structural cartoons illustrate native and cold-denatured structures for apomyoglobin with the A, G, and H helices indicated.[31,51,52] (B) Free energy cross-section $\Delta G(T=T_f,\mathrm{Rs})$ at the refolding temperature following the T-jump. This is the surface on which the fast kinetics occur. In the presence of a barrier, several scenarios are possible. (1) The cold-denatured state is more extended than the denatured state at T_f; the protein rapidly contracts and then folds more slowly over the barrier. (2) The two states have a comparable local minimum, and no contraction is observed prior to activated kinetics. (3) The cold-denatured state is a transition state at T_f, and both folding and unfolding kinetics are observed. (4) The cold-denatured state already has the transition-state contacts necessary for folding at higher temperature, and rapid type 0 downhill folding occurs. In all of these cases, some reverse reaction of course also contributes to the observed rates. Scenarios without a barrier are possible if the entropy ("width") of the folding funnel is compensated by the enthalpy ("depth") of the funnel.

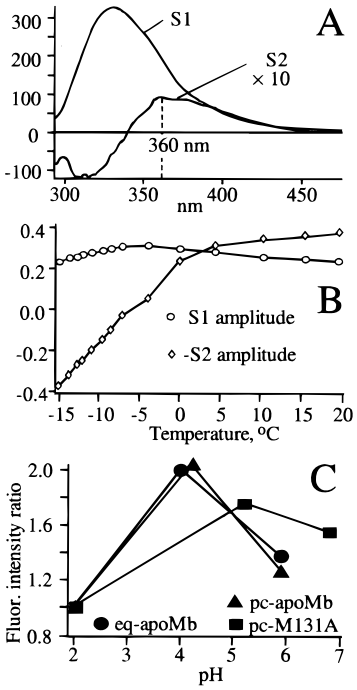

FIGURE 3. Fluorescence properties of *eq*-apoMb. (A) the two significant singular value components of the fluorescence between −15 and 20 °C. S1 = average fluorescence spectrum, while S2 = temperature dependence (more >350 nm solvated fluorescence at low *T*). (B) SVD components as a function of temperature. S2 shows the onset of cold denaturation near 0 °C, while S1 shows hyperfluorescence during the initial phase of the unfolding transition. (C) Sensitivity of apoMb fluorescence to removal of the specific methionine 131−tryptophan 14 interaction. The methionine 131-free mutant shows less quenching in the native state and significantly less hyperfluorescence.

denaturation transition appears as a sharp two-state transition, and circular dichroism indicates little residual secondary structure. Following a T-jump to 5−20 °C, observation of phosphoglycerate kinase fluorescence on a 1−2000 μs time scale reveals a continuum of kinetic phases ranging from 10 μs to 6 ms.[37,64] Such multiscale kinetics potentially indicate downhill folding scenarios, where entropy loss and enthalpic driving forces balance out.[49,64]

The third protein in Table 1 is apoMb. We discuss it in detail to address the finer points of T-jump folding experiments (Figure 4). We begin with some of the difficulties associated with T-jump fluorescence detection and their resolution.

Even a $^1/_{10}$ k_BT jump between similar initial and final solvent densities (around 4 °C) can launch pressure waves or generate gas bubbles which obscure folding dynamics. Although collection in a large solid angle makes fluorescence detection less sensitive to such artifacts than direct absorption (transmission) measurements, we do observe large oscillations in fluorescence intensity very different from the folding signals under extreme conditions (ΔT > 30 °C, or far from density maximum of aqueous solvent). Sample degassing and a two-beam counterpropagating delayed pump geometry with a large ratio of pump to probe beam diameter are used to eliminate such artifacts

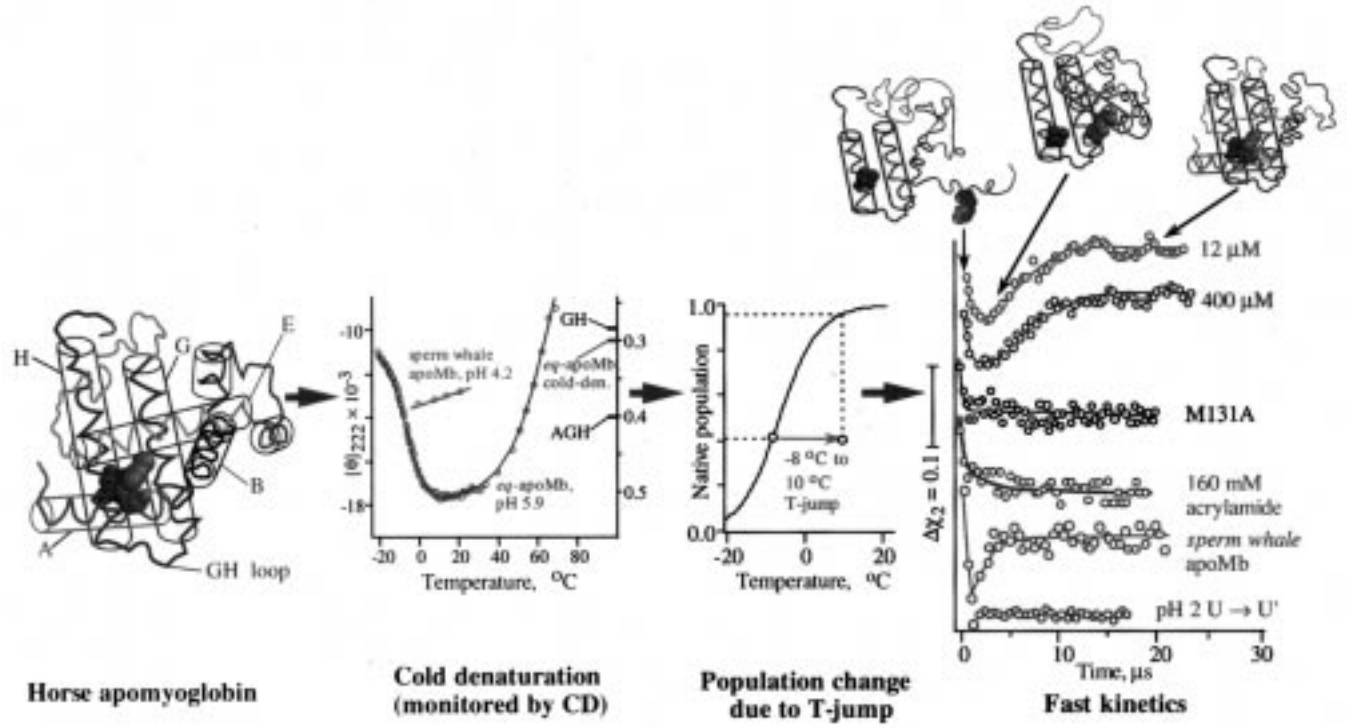

FIGURE 4. Structure of apoMb with the A-helix (red), GH helical hairpin (blue), and residues tryptophan 14 (red) and methionine 131 (blue). The temperature-dependent far-UV CD at 222 nm for horse apoMb shows helical fraction (right vertical axis) and key reference points. The solid line represents a three-state thermodynamic fit (cold-denatured, heat-denatured, and native). The resulting native population vs temperature plot shows a typical T-jump highlighted in red.[31] Fast kinetic data are plotted using the χ_2 described in the text (conditions of Table 1 unless noted). Larger values of χ_2 indicate more tryptophan quenching. Kinetic data were fitted using a double exponential with time constants τ_1 = 250−400 ns (fast "protective phase") and τ_2 = 4−17 μs (quenching phase). Other transients illustrate (top to bottom) concentration independence of the kinetics, absence of observed dynamics when methionine 131 is removed, tuning of the quenching phase by addition of acrylamide to the buffer, presence of the quenching phase in a tryptophan 7 to phenylalanine mutant, and absence of observed dynamics during U → U′ transitions at pH 2.

(Figure 1).[36] As a result, tryptophan control solutions and pH 2 apoMb control solutions (protein remains unfolded at any temperature) show no significant dynamics following T-jumps (Figure 4). Dimerization or aggregation could also result in fluorescence changes unrelated to folding kinetics. Figure 4 shows that the observed refolding dynamics of apoMb are essentially constant over a factor of 35 range in concentration.

Jennings and Wright[6] have previously observed a burst phase in their millisecond time resolution stopped-flow/CD detected experiments, during which the protein acquired 70% of its native helical structure. Their NMR experiments also showed significant protection of the A, G, and H amide protons. Our experiments have resolved the dynamics within this burst phase.

The T-jump induced refolding of apoMb shows two kinetic phases (Figure 4): a 250 ns phase during which the fluorescence lifetime increases ("protective" phase), and a 4−17 μs "quenching" phase, whose observed rate decreases with solvent viscosity.[9] This microsecond phase depends only weakly on temperature between 5 and 20 °C and corresponds to a 0.3 ns shortening of the tryptophan fluorescence lifetime and 20% lower fluorescence intensity. No further kinetics of significant amplitude were observed up to 2 ms, where stopped-flow experiments indicate a nativelike AGH core.

In the native AGH core, tryptophan 14 (A helix) and methionine 131 (a strong Dexter quencher near the GH turn) are in dipolar contact.[51] We assign the microsecond quenching phase to the formation of a near-native contact between the tryptophan in the nascent A helix and the methionine at the other end of the primary sequence. Since some GH structure already exists in the D_C ensemble[31] and Dexter quenching is short-range[43] (section III), this corresponds to the time required for the nascent A helix to diffuse to the GH loop and to closely dock against it. The observed microsecond time scale lies at the lower end of what is expected for AGH core formation with an A−GH connecting loop size of ≈80 residues,[11,25] especially given the many other a priori alternatives for the folding protein (such as docking of B through E helices against the GH loop prior to formation of the nativelike core).

Several observations confirm the above assignment. The microsecond phase is the *only* quenching phase observed up to 2 ms, at which point stopped-flow experiments[6] show that the AGH core has formed even from an almost completely unfolded ensemble.[65] The specificity of the methionine−tryptophan quenching is illustrated in Figure 3: although horse and sperm whale apoMb differ by 20 sequence mutations, they share the native methionine−tryptophan contact[51,66] and show very similar fluo-

rescence properties during denaturation.[31,44] In contrast, a sperm whale apoMb methionine 131 to alanine mutant shows only weak hyperfluorescence and quenching (Figure 3).[44] Its T-jump transient (Figure 4) shows the rapid 250 ns phase, but no significant microsecond quenching phase as observed in the wild-type proteins. A sperm whale apoMb mutant with Trp 7 removed but Trp 14 intact also shows a microsecond quenching phase, which is smaller in keeping with the fact that its cold denaturation is not as complete.

The picture is rounded out by two more measurements. Shown in Figure 4 is a U → U′ pH 2 T-jump where the initial and final states are both unfolded. There is only a very small ≈1 μs quenching phase present, indicating that the slight polymer backbone contraction expected under fully denaturing conditions with increasing temperature does not lead to specific quenching interactions. In a final test, the microsecond quenching phase can be titrated away as the solvent concentration of the tryptophan quencher acrylamide is raised from 0 to 150 mM (Figure 4): this is the point where quenching of the tryptophans in the AGH core equals the nonspecific solvent quenching interaction. The fact that the microsecond phase can even be made slightly protective at higher acrylamide concentrations indicates that there is significant solvent exclusion from the AGH core after just a few microseconds. In conclusion, this fast phase leading to the AGH core is not just barely sub-microsecond in duration, but turns out to be a factor of 100 faster than the stopped-flow time resolution. These results finally provide direct evidence for fast core formation, as well as useful constraints for refining theoretical models.[67−69]

The faster phase that precedes the protective AGH formation phase is more difficult to assign (Figure 4).[35] It is clearly due to a local collapse process around tryptophan 14 (and to a lesser extent, tryptophan 7) which precedes AGH core formation. We interpret it as a combination of rapidly formed nonnative tertiary contacts inducing formation of the full A helix.

A number of observations lead to this assignment. The 250 ns phase remains "protective" (longer fluorescence lifetime) upon addition of acrylamide to the solution. It is also present in the methionine 131 to alanine mutant and in the tryptophan 7-free mutant of *pc*-apoMb. Furthermore, the time scale is consistent with helix formation rates.[20,21,70] Finally, our steady-state data on the cold-denatured ensemble show that the tertiary contacts between the A-helix in *eq*-apoMb and the GH interface are gone in the cold-denatured state and that the A peptide when isolated does not acquire helical structure under our cold-denaturation conditions.[31] The latter fact leads us to believe that helix formation must be accompanied at the very least by formation of nonspecific tertiary contacts among hydrophobic side chains, which could shift the coil−helix transition free energy of the amphiphilic A helix to a value favorable for folding.

However, a definitive assignment requires the observation of such "nonspecific" collapse and formation of helical structure by infrared or circular dichroism experiments. Fluorescence quenching via specific tertiary interactions alone leaves other possibilities open. For instance, since two phases are observed experimentally, the data can be fitted to a general three-state mechanism:[35]

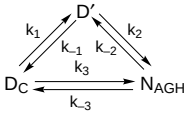

(2)

In our above explanation of the data, D′ is a nonspecifically collapsed state with A helix present, rapidly formed from D_C, which does not directly convert to N_{AGH} ($k_{+3} = k_{-3} = 0$). However, equally good fits can be obtained if $k_{+2} = k_{-2} = 0$, in which case D′ could be some misfolded state competing with the refolding kinetics. This corresponds to the left-going arrow in Figure 2, if the temperature jump promotes the ensemble D_C to a state near the barrier at the final refolding temperature. The ambiguity inherent in eq 2 for scenarios beyond two-state equilibria cannot be overemphasized. Only an exhaustive mapping of the folding phase diagram as a function of temperature and denaturant concentration can lead to an unambiguous resolution and assignment of folding phases to specific kinetic schemes. Although efforts in this direction have begun in our and other groups, and some transition-state ensembles have been carefully characterized,[34] much remains to be done in this regard in fast folding experiments.

V. Outlook

T-jump techniques have opened up a new time scale, covering the previously hidden 6 orders of magnitude from milliseconds to nanoseconds and beyond. The early experiments[7−9,11,21,25−27] demonstrate that the combination of kinetics and steady-state structural observations can unravel the nature of the very first steps during protein folding or unfolding.

The apoMb experiments raise several issues. Is a nonspecific "precollapse" necessary for helix formation preceding AGH core formation? This can be addressed by fluorescence experiments using the Förster mechanism, for example quenching of tryptophan 14 by chemically modified tyrosine 146: if there is a very rapid collapse, it should reveal itself as a quenching phase during which the tryptophan−tyrosine distance rapidly shrinks from >40 to <20 Å. Helix formation could be verified by direct measures of secondary structure such as circular dichroism or infrared amide spectroscopy, which has already been used to study rapid apomyoglobin unfolding.[12] Do other domains fold at different rates? Comparison with NMR experiments indicates that the heme binding CDEF domain folds far more slowly than the AGH domain. Perhaps this indicates that the residue composition of functional domains compromises folding at the expense of activity, while mainly structural domains are better optimized for folding. Yet other time scales may reveal themselves if tryptophan mutants of the B through F helices are investigated.

On a more general level, one would like to understand how universal submillisecond folding is, and what common features emerge at early times. Some proteins such as apoMb and cytochrome *c* appear to form terminal secondary structure and tertiary contacts first, resulting in a "ring" topology for the folding backbone. It appears that local signals play an important role in these and in other proteins such as PGK, which forms secondary structure in under 5 ms[18,40,62,63] in a collapse process with several time scales.[37]

In other cases, global signals among residues greatly separated in primary sequence could play an important role.[71,72] This leads to a slow and highly activated first step during folding. Knowledge of such a transition state is valuable because it greatly restricts the palette of available structures during the following downhill folding to the native state. However, the transition state alone cannot fully constrain the subsequent dynamics for an object as complex as a protein. Particularly an early transition state leaves the protein with many dynamical options during the final downhill process. In that respect, initiation of "type 0" folding from ensembles near the transition state, as suggested in Figure 2, is of particular importance: it can tell us how the transition state sets up the protein for acquisition of the native fold.

During the next several years we will see a proliferation of discoveries in protein folding kinetics studied by T-jump and the other fast techniques described in this issue, as continual improvements of lasers and detection technology, the development of hybrid systems employing multiple detection schemes, and the use of site-directed mutagenesis provide a fresh window onto the forces that control protein folding.

The authors are grateful for support from the National Science Foundation, the Lucile and David Packard Foundation, and the American Chemical Society Petroleum Research Fund. M.G. was a Cottrell Scholar and a Dreyfus and Sloan Fellow and J.S. was a Procter and Gamble Scholar. Steady-state measurements were performed at the UIUC Laboratory of Fluorescence Dynamics.

References

(1) Bryngelson, J. D.; Wolynes, P. G. *Proc. Natl. Acad. Sci. U.S.A.* **1987**, *84*, 7524−7528.
(2) Frauenfelder, H.; Sligar, S. G.; Wolynes, P. G. *Science* **1991**, *254*, 1598−1603.
(3) Dill, K. A. *Biochemistry* **1990**, *29*, 7134−7155.
(4) Boczko, E. M.; Brooks, C. L. I. *Science* **1995**, *269*, 393−396.
(5) Briggs, M.; Roder, H. *Proc. Natl. Acad. Sci. U.S.A.* **1992**, *89*, 2017−2021.
(6) Jennings, P.; Wright, P. *Science* **1993**, *262*, 892−895.
(7) Huang, G. S.; Oas, T. G. *Proc. Natl. Acad. Sci. U.S.A.* **1995**, *92*, 6878−6882.
(8) Nölting, B.; Golbik, R.; Fersht, A. R. *Proc. Natl. Acad. Sci. U.S.A.* **1995**, *92*, 10668−10672.
(9) Ballew, R. M.; Sabelko, J.; Gruebele, M. *Proc. Natl. Acad. Sci. U.S.A.* **1996**, *93*, 5759−5764.
(10) Pascher, T.; Chesick, J. P.; Winkler, J. R.; Gray, H. B. *Science* **1996**, *271*, 1558−1560.
(11) Chan, C.; Hu, Y.; Takahashi, S.; Rousseau, D. L.; Eaton, W. A.; Hofrichter, J. *Proc. Natl. Acad. Sci. U.S.A.* **1997**, *94*, 1779−1784.
(12) Gilmanshin, R.; Williams, S.; Callender, R. H.; Woodruff, W. H.; Dyer, R. B. *Proc. Natl. Acad. Sci. U.S.A.* **1997**, *94*, 3709−3713.
(13) Hagen, S. J.; Hofrichter, J.; Eaton, W. A. *J. Phys. Chem. B* **1997**, *101*, 2352−2365.
(14) Yeh, S.; Takahashi, S.; Fan, B.; Rousseau, D. L. *Nat. Struct. Biol.* **1997**, *4*, 51−56.
(15) Chaffotte, A. F.; Guillou, Y.; Goldberg, M. E. *Biochemistry* **1992**, *31*, 9693−9702.
(16) Itzhaki, L. S.; Evans, P. A.; Dobson, C. M.; Radford, S. E. *Biochemistry* **1994**, *33*, 5212−5220.
(17) Roder, H.; Elöve, G.; Englander, S. W. *Nature* **1988**, *335*, 700−704.
(18) Hosszu, L. L. P.; Craven, C. J.; Parker, M. J.; Lorch, M.; Spencer, J.; Clarke, A. R.; Waltho, J. P. *Nat. Struct. Biol.* **1997**, *4*, 801−804.
(19) Bryngelson, J. D.; Onuchic, J. N.; Socci, N. D.; Wolynes, P. G. *Proteins: Struct., Funct., Genet.* **1995**, *21*, 167−195.
(20) Hammes, G. G.; Roberts, P. B. *J. Am. Chem. Soc.* **1969**, *91*, 1812−1816.
(21) Williams, S.; Causgrove, T. P.; Gilmanshin, R.; Fang, K. S.; Callender, R. H.; Woodruff, W. H.; Dyer, R. B. *Biochemistry* **1996**, *35*, 691−697.
(22) Muñoz, V.; Thompson, P. A.; Hofrichter, J.; Eaton, W. A. *Nature* **1997**, *390*, 196−199.
(23) Hagen, S. J.; Hofrichter, J.; Szabo, A.; Eaton, W. A. *Proc. Natl. Acad. Sci. U.S.A.* **1996**, *93*, 11615−11617.
(24) Lewis, J. W.; Goldbeck, R. A.; Kliger, D. S.; Xie, X.; Dunn, R. C.; Simon, J. D. *J. Phys. Chem.* **1992**, *96*, 5243−5254.
(25) Jones, C. M.; Henry, E. R.; Hu, Y.; Chan, C.; Luck, S. D.; Bhuyan, A.; Roder, H.; Hofrichter, J.; Eaton, W. A. *Proc. Natl. Acad. Sci. U.S.A.* **1993**, *90*, 11860−11864.
(26) Phillips, C. M.; Mizutani, Y.; Hochstrasser, R. M. *Proc. Natl. Acad. Sci. U.S.A.* **1995**, *92*, 7292−7296.
(27) Mines, G. A.; Pascher, T.; Lee, S. C.; Winkler, J. R.; Gray, H. B. *Chem. Biol.* **1996**, *3*, 491−497.
(28) Privalov, P. L. *Crit. Rev. Biochem. Mol. Biol.* **1990**, *25*, 281−305.
(29) Zhang, J.; Peng, X.; Jonas, A.; Jonas, J. *Biochemistry* **1995**, *34*, 8631−8641.
(30) Petrescu, A.; Receveur, V.; Calmettes, P.; Durand, D.; Desmadril, M.; Roux, B.; Smith, J. C. *Biophys. J.* **1997**, *72*, 335−342.
(31) Sabelko, J.; Ervin, J.; Gruebele, M. *J. Phys. Chem. B* **1998**, *102*, 1806−1819.
(32) Eigen, M.; Maeyer, L. D. In *Technique of Organic Chemistry*; Weissberger, A., Ed.; Interscience: New York, 1963; pp 895−1054.
(33) Turner, D. H.; Flynn, G. W.; Sutin, N.; Beitz, J. V. *J. Am. Chem. Soc.* **1972**, *94*, 1554−1559.
(34) Nölting, B.; Golbik, R.; Neira, J. L.; Soler-Gonzalez, A. S.; Schreiber, G.; Fersht, A. R. *Proc. Natl. Acad. Sci. U.S.A.* **1997**, *94*, 826−830.
(35) Ballew, R. M.; Sabelko, J.; Gruebele, M. *Nat. Struct. Biol.* **1996**, *3*, 923−926.
(36) Ballew, R. M.; Sabelko, J.; Reiner, C.; Gruebele, M. *Rev. Sci. Instrum.* **1996**, *67*, 3694−3699.
(37) Gruebele, M.; Sabelko, J.; Ervin, J. *Biophys. J.* **1998**, *74*, M-PM-B6.
(38) Anfinrud, P. A.; Han, C.; Hochstrasser, R. M. *Proc. Natl. Acad. Sci. U.S.A.* **1989**, *86*, 8387−8391.
(39) Takahashi, S.; Yeh, S.; Das, T. K.; Chan, C.; Gottfried, D. S.; Rousseau, D. L. *Nat. Struct. Biol.* **1997**, *4*, 44−50.
(40) Lillo, M. P.; Beechem, J. M.; Szpikowska, B. K.; Sherman, M. A.; Mas, M. T. *Biochemistry* **1997**, *36*, 11261−11272.

(41) Rischel, C.; Thyberg, P.; Rigler, R.; Poulsen, F. M. *J. Mol. Biol.* **1996**, *257*, 877−885.
(42) Steiner, R. F.; Kirby, E. P. *J. Phys. Chem.* **1969**, *73*, 4130−4135.
(43) Gilst, M. v.; Tang, C.; Roth, A.; Hudson, B. *J. Fluoresc.* **1994**, *4*, 203−207.
(44) Kay, M.; Baldwin, R. *Nat. Struct. Biol.* **1996**, *3*, 439−445.
(45) Kuroda, Y.; Kidokoro, S.; Wada, A. *J. Mol. Biol.* **1992**, *223*, 1139−1153.
(46) Nishii, I.; Kataoka, M.; Tokunaga, F.; Goto, Y. *Biochemistry* **1994**, *33*, 4903−4909.
(47) Gast, K.; Damaschun, G.; Damaschun, H.; Misselqitz, R.; Zirwer, D. *Biochemistry* **1993**, *32*, 7747−7752.
(48) Nash, D. P.; Jonas, J. *Biochem. Biophys. Res. Commun.* **1997**, *238*, 289−291.
(49) Onuchic, J. N.; Luthey-Schulten, Z.; Wolynes, P. G. *Annu. Rev. Phys. Chem.* **1997**, *48*, 545−600.
(50) Wolynes, P. G.; Onuchic, J. N.; Thirumalai, D. *Science* **1995**, *267*, 1619−1620.
(51) Cocco, M. J.; Lecomte, J. T. J. *Biochemistry* **1990**, *29*, 11067−11072.
(52) Eliezer, D.; Wright, P. E. *J. Mol. Biol.* **1996**, *263*, 531−538.
(53) Gast, K.; Damaschun, H.; Misselwitz, R.; Müller-Frohne, M.; Zirwer, D.; Damaschun, G. *Eur. Biophys. J.* **1994**, *23*, 297−605.
(54) Hughson, F.; Wright, P.; Baldwin, R. *Science* **1990**, *249*, 1544−1548.
(55) Nishii, I.; Kataoka, M.; Goto, Y. *J. Mol. Biol.* **1995**, *250*, 223−238.
(56) Griko, Y. V.; Privalov, P. L.; Venyaminov, S. Y.; Kutyshenko, V. P. *J. Mol. Biol.* **1988**, *220*, 127−138.
(57) Damaschun, G.; Damaschun, H.; Gast, K.; Misselwitz, R.; Müller, J. J.; Pfeil, W.; Zirwer, D. *Biochemistry* **1993**, *32*, 7739−7746.
(58) Elöve, G.; Chaffotte, A.; Roder, H.; Goldberg, M. *Biochemistry* **1992**, *31*, 6876−6883.
(59) Colón, W.; Roder, H. *Nat. Struct. Biol.* **1996**, *3*, 1019−1025.
(60) Pinheiro, T. J. T.; Elöve, G.; Watts, A.; Roder, H. *Biochemistry* **1997**, *36*, 13122−13132.
(61) Yeh, S.; Rousseau, D. L. *Nat. Struct. Biol.* **1998**, *5*, 222−228.
(62) Lillo, M. P.; Szpikowska, B. K.; Mas, M. T.; Sutin, J. D.; Beechem, J. M. *Biochemistry* **1997**, *36*, 11273−11281.
(63) Lillo, P.; Mas, M. T.; Beechem, J. M. *Biophys. J.* **1998**, *74*, Tu-Pos-130.
(64) Brooks, C. L. I.; Gruebele, M.; Onuchic, J. N.; Wolynes, P. G. *Proc. Natl. Acad. Sci. U.S.A.*, in press.
(65) Eliezer, D.; Yao, J.; Dyson, H. J.; Wright, P. E. *Nat. Struct. Biol.* **1998**, *5*, 148−155.
(66) Lecomte, J. T. J.; Kao, Y.; Cocco, M. J. *Proteins: Struct., Funct., Genet.* **1996**, *25*, 267−285.
(67) Karplus, M.; Weaver, D. L. *Nature* **1976**, *260*, 404−406.
(68) Bashford, D.; Cohen, F. E.; Karplus, M.; Kuntz, I. D.; Weaver, D. L. *Proteins: Struct., Funct., Genet.* **1988**, *4*, 211−227.
(69) Pappu, R. V.; Weaver, D. L. *Protein Sci.* **1998**, *7*, 480−490.
(70) Poland, D.; Scheraga, H. A. *J. Chem. Phys.* **1966**, *45*, 2071−2090.
(71) Abkevich, A. I.; Gutin, A. M.; Shakhnovich, E. I. *J. Mol. Biol.* **1995**, *252*, 460−471.
(72) Sosnick, T. R.; Shtilerman, M. D.; Mayne, L.; Englander, S. W. *Proc. Natl. Acad. Sci. U.S.A.* **1997**, *94*, 8545−8550.
(73) Onuchic, J. N.; Socci, N. D.; Luthey-Schulten, Z.; Wolynes, P. G. *Folding Des.* **1996**, *1*, 441−450.

AR970083X